PROTEINS: Structure, Function, and Genetics 40:58–70 (2000)

Lower Kinetic Limit to Protein Thermal Stability: A Proposal Regarding Protein Stability In Vivo and Its Relation With Misfolding Diseases

Isabel M. Plaza del Pino, Beatriz Ibarra-Molero, and Jose M. Sanchez-Ruiz*
Facultad de Ciencias, Departamento de Quimica Fisica, Universidad de Granada, Granada, Spain

ABSTRACT **In vitro thermal denaturation experiments suggest that, because of the possibility of irreversible alterations, thermodynamic stability (i.e., a positive value for the unfolding Gibbs energy) does not guarantee that a protein will remain in the native state during a given timescale. Furthermore, irreversible alterations are more likely to occur in vivo than in vitro because (a) some irreversible processes (e.g., aggregation, "undesirable" interactions with other macromolecular components, and proteolysis) are expected to be fast in the "crowded" cellular environment and (b) in many cases, the relevant timescale in vivo (probably related to the half-life for protein degradation) is expected to be longer than the timescale of the usual in vitro experiments (of the order of minutes). We propose, therefore, that many proteins (in particular, thermophilic proteins and "complex" proteins systems) are designed (by evolution) to have significant kinetic stability when confronted with the destabilizing effect of irreversible alterations. We show that, as long as these alterations occur mainly from non-native states (a Lumry-Eyring scenario), the required kinetic stability may be achieved through the design of a sufficiently high activation barrier for unfolding, which we define as the Gibbs energy barrier that separates the native state from the non-native ensemble (unfolded, partially folded, and misfolded states) in the following generalized Lumry-Eyring model:**

Native State ↔ Non-Native Ensemble →

Irreversibly Denatured Protein

Finally, using familial amyloid polyneuropathy (FAP) as an illustrative example, we discuss the relation between stability and amyloid fibril formation in terms of the above viewpoint, which leads us to the two following tentative suggestions: (a) the hot spot defined by the FAP-associated amyloidogenic mutations of transthyretin reflects the structure of the transition state for unfolding and (b) substances that decrease the in vitro rate of transthyretin unfolding could also be inhibitors of amyloid fibril formation. Proteins 2000;40:58–70.

Key words: denaturation; irreversibility; energetics; thermophilic proteins; amyloids

INTRODUCTION

Thermal denaturation of proteins is often discussed in terms of the Lumry-Eyring model[1–3]:

$$N \leftrightarrow U \rightarrow F \quad (1)$$

where the N is the native state, U is the unfolded state, and F stands for a protein state (using here the word *state* in a very general sense), which results from the irreversible alteration of U: the final state. A number of processes may be responsible for this irreversible alteration in vitro, including aggregation, autolysis, and covalent alteration of residues.[4] It is worth noting here that the words *reversible* and *irreversible*, as used in the literature on protein stability (and in classical thermodynamics!), may have different, although related, meanings. Here, we use the word *irreversible* to describe the step $U \rightarrow F$ (and the overall denaturation process, starting with N and ending with F) meaning that, under the conditions in which denaturation is being studied, the final state is unable to "return" to N or U. (It is, of course, conceivable that, once a denaturation experiment is over, a researcher be able to recover the native state by using a more or less ingenious procedure; this, however, would not be relevant to the analysis of protein stability.) On the other hand, the step $N \leftrightarrow U$ is assumed in the model to proceed in both ways and is, therefore, labeled reversible. Note that the $U \rightarrow F$ conversion must be necessarily described in a rate equation, whereas the relative amounts of N and U at equilibrium are determined by the unfolding thermodynamics; of course, the folding-unfolding equilibrium may not be reached under certain experimental conditions (e.g., fast temperature scanning; see Freire et al.[3]), and, conse-

Abbreviations: CI-2, chymotripsin inhibitor 2; DSC, differential scanning calorimetry; HEW, hen egg white; FAP, familial amyloid polyneuropathy; LEM, linear extrapolation method; TTR, transthyretin; WT, wild type.

Grant sponsor: DGES (Spanish Ministry of Education and Culture); Grant number: PB96-1439.

Beatriz Ibarra-Molero's present address is Department of Chemistry, Penn State University, University Park, Pennsylvania.

*Correspondence to: Facultad de Ciencias, Departamento de Quimica Fisica. Fuentenueva s/n. 18071-Granada, Spain. E-mail: sanchezr@goliat.ugr.es

Received 8 November 1999; Accepted 10 February 2000

quently, it may be necessary to take into account the folding-unfolding kinetics in denaturation data analyses[3] and theoretical simulations (as we will do, in this work).

Clearly, the Lumry-Eyring model of Eq. 1 is the simplest model that takes into account the essential features of irreversible protein denaturation, and more complex situations may be found in practice (e.g., the unfolding step might involve significantly populated intermediate states). A useful and reasonable way to generalize the Lumry-Eyring model is described in the following paragraph.

Recent theoretical studies (the so-called "new-view" of protein folding; for reviews, see Refs. 5–7) describe protein folding-unfolding processes in terms of the energy landscape (the multidimensional surface of energy versus conformational degrees of freedom), emphasize the difficulty in defining a single reaction coordinate for folding, and point out that individual chain may fold by multiple pathways. We believe, nevertheless, that it is still acceptable to assume that there is at least one well-defined kinetic barrier (in the transition-state-theory sense) separating the native state from all other non-native states. This view is supported by the fact that, on transfer to strongly denaturing conditions, native proteins unfold much more slowly than intermediate states (likely partially folded or misfolded protein; see Privalov[8]), a property that is the basis of the well-known double-jump, unfolding assays for the amount of native proteins.[9–12] Accordingly, we write the general Lumry-Eyring model as

$$N \leftrightarrow \{\textit{Non-native ensemble}\} \rightarrow F \qquad (2)$$

where the non-native ensemble includes unfolded, partially unfolded, and misfolded protein states; we refer to the kinetic barrier separating the native state from the non-native ensemble simply as the "activation barrier for unfolding." The scheme shown in Eq. 2 reveals what we believe is the main feature of Lumry-Eyring models: the assumption that the native state is comparatively safe and that, for the protein to become susceptible to irreversible alterations, it must cross the activation barrier for unfolding. For the sake of simplicity, the illustrative computer simulations reported in this work are based on the simplest form of the Lumry-Eyring model (Eq. 1); however, we eventually discuss the results obtained in terms of the more general interpretation given in Eq. 2.

Whether irreversible alterations occur significantly in a specific experimental case depends on several factors. First, in vitro experiments (reviewed below) suggest that complex protein systems (e.g., membrane proteins and oligomeric proteins) are more prone to irreversible alterations than low molecular weight model proteins. Second, because irreversible alterations are kinetic processes described by rate equations, the relevant experimental timescale plays also a fundamental role; thus, for a given protein, irreversible alterations may not take place during the usual in vitro thermal denaturation experiments (timescale of the order of minutes, usually), but still irreversible alterations may determine the long-term stability of that protein at room temperature (e.g., shelf-life of protein pharmaceuticals), because the timescale involved is now much longer (i.e., weeks, months, years, etc.). Finally, another important factor is the environment: irreversible alterations can sometimes be avoided under the carefully controlled conditions (e.g., buffer, pH, ionic strength, and protein concentration) of the in vitro thermal denaturation experiments. This factor contrasts sharply with the environment proteins found in vivo (or even in some technological applications); thus, in a crowded cellular environment we may expect that irreversible alterations of non-native states (proteolytic cleavage, aggregation, or strong interactions with other macromolecular systems) will occur fast. In fact, thermal denaturation experiments with whole cells or isolated cellular organelles[13–17] show irreversible protein denaturation.

Fundamental studies of protein folding-unfolding energetics have (reasonably) focused on reversible unfolding processes. As mentioned above, this usually involves performing in vitro denaturation studies with diluted solutions of low molecular weight model proteins and, furthermore, using solvent conditions at which irreversible processes are found not to occur significantly for the given protein under study. However, even in the simple environment and the comparatively short timescale of the usual in vitro experiments, irreversible processes often occur, despite all precautions. The systematic analysis of in vitro, irreversible denaturation of proteins begun some 12 years ago and, after a significant number of experimental studies, a somewhat surprising picture has emerged. Thus, in many cases,[18–46] irreversible thermal denaturation of proteins (as monitored by differential scanning calorimetry [DSC], e.g.) can be phenomenologically described on the basis of a simple two-state irreversible model:

$$N \xrightarrow{k_{ap}} F \qquad (3)$$

in which only the native and final states are significantly populated and the conversion from N to F is determined by a strongly temperature-dependent, first-order rate constant (k_{ap}). Theoretical analysis[2] shows that this two-state model may be considered as a limiting case of the Lumry-Eyring model. According to this interpretation, the two-state irreversible model must not be taken to mean that the native state undergoes the irreversible alteration leading to F: the irreversible step is still $U \rightarrow F$ (using the simpler scheme of Eq. 1), but it is fast and the overall denaturation process occurs under conditions (temperature range) at which the amount of unfolded state (or non-native protein, in general) is very low. Then, the operational thermal stability of the protein is decreased by the occurrence of irreversible alterations, in the sense that the overall denaturation process is fast (occurs in a given relevant timescale) at temperatures lower than the thermodynamic denaturation temperature (temperature at which the unfolding Gibbs energy change is zero). In other words, thermodynamic stability (i.e., a positive value for unfolding Gibbs energy) does not prevent the protein from undergoing irreversible denaturation in a given timescale. This "kinetic stability" problem should be particularly

TABLE I. Parameters Used in the Lumry-Eyring Simulations[†]

	Lysozyme	Barnase	CI-2
T_m (K)	350.1 (pH 4.5, AcNa 50 mM[11])	328.0 (pH 6.3, Mes 50 mM[51])	353.2 (pH 6.3, Mes 50 mM[79])
ΔH_m (kJ/mol)	577	606	312
ΔC_p (kJ · K^{-1} · mol^{-1})	6.5	7.2	3.2
$E_{N\rightarrow U}$ (kJ/mol)	195	253	154
T^* (K)	335.9	312.5	321.0

[†]The pH and buffer conditions given in the T_m file are those to which the T_m values and kinetic parameters correspond, and the superior numbers are the literature references relevant for the T_m values.

acute in vivo, because (a) as mentioned above, irreversible alterations of nonnative proteins are expected to be fast in vivo and (b) the relevant in vivo timescale for a protein is likely to be given by the half-life for protein degradation, which, in some cases, is of the order of several days or longer.[47]

The above reasoning leads us to hypothesize that, in the same manner that evolution has designed proteins to have significant thermodynamic stability at physiological temperature (a positive, but not too large, unfolding Gibbs energy; see Doig and Williams[48]), many proteins are also designed to have significant kinetic stability when confronted with the destabilizing effect of irreversible alterations (the likely situation in vivo). The main purpose of this work is to investigate theoretically how this kinetic stability may be attained. To do so, we selected three model proteins (HEW lysozyme, barnase, and chymotrypsin inhibitor 2[CI-2]) whose denaturation in vitro is usually little affected by irreversible alterations, and we theoretically determined how their thermal stability (as monitored by DSC) would be affected if they are placed in an environment in which irreversible alterations occur readily (which may well be, in fact, the situation these proteins must confront in vivo).

RESULTS AND DISCUSSION

Fully Kinetic Analysis of the Lumry-Eyring Model

Our theoretical simulations are based on the fully kinetic analysis of the Lumry-Eyring model[49]; that is, we do not assume the unfolding step to be at equilibrium, but we take into account the kinetic of the folding and unfolding processes, together with the kinetics of the irreversible step. Thus, we use the following equations:

$$\frac{dX_N}{dT} = \frac{1}{v}\cdot(-k_{N\rightarrow U}\cdot X_N + k_{U\rightarrow N}\cdot X_U) \quad (4)$$

$$\frac{dX_U}{dT} = \frac{1}{v}\cdot(k_{N\rightarrow U}\cdot X_N - k_{U\rightarrow N}\cdot X_U - k_{U\rightarrow F}\cdot X_U) \quad (5)$$

$$\frac{dX_F}{dT} = \frac{1}{v}\cdot k_{U\rightarrow F}\cdot X_U \quad (6)$$

$$C_P^{EX} = -\Delta H\cdot\frac{dX_N}{dT} + (1 - X_N)\cdot\Delta C_P \quad (7)$$

where the meaning of the symbols is as follows: X_N, X_U, and X_F are the populations of the states *N, U,* and *F*; $k_{N\rightarrow U}$, $k_{U\rightarrow N}$ and $k_{U\rightarrow F}$ are the first-order rate constants for the processes $N\rightarrow U$, $U\rightarrow N$, and $U\rightarrow F$ of the Lumry-Eyring model; ΔH is the unfolding enthalpy change, which is assumed to change with temperature (T) according to a constant unfolding heat capacity change, ΔC_P; C_P^{EX} is the excess heat capacity taking the native state as reference. Eqs. 4–6 are the kinetic equations of the Lumry-Eyring model for an experiment in which temperature is changed with time according to a constant scanning rate (v), and Eq. 7 allows us to compute the corresponding DSC transition, once the system of three differential equations (Eqs. 4–6) has been integrated.

We use several simplifying assumptions in our calculations:

- A temperature-independent rate constant for the irreversible step. It will be made clear by our analysis that this does *not* imply that rate constant for the overall irreversible denaturation (k_{ap}) is temperature independent.
- A zero enthalpy change for the irreversible step ($U\rightarrow F$).
- A temperature-independent heat capacity change for unfolding; that is, we neglect the (comparatively small) effect of temperature on ΔC_p and, therefore, assume that the unfolding enthalpy changes linearly with temperature:

$$\Delta H = \Delta H_m + \Delta C_p\cdot(T - T_m) \quad (8)$$

where ΔH_m is the unfolding enthalpy change at the "equilibrium denaturation temperature" (the temperature, T_m, at which the unfolding equilibrium constant equals unity). The values used for T_m (and the pH and buffer conditions to which they correspond) are given in Table I for the three proteins under study. The values we have used for ΔH_m and ΔC_p (collected in Table I) are those determined from the fitting of Eq. 7 to the ΔH versus T data (within the 5–75°C range) given in the review by Makhatadze and Privalov[50] or, in the case of barnase, those given in Johnson and Fersht.[51]

The above assumptions are only introduced for the sake of simplicity and do not affect any of the general results and conclusions of our analysis. On the other hand, it is

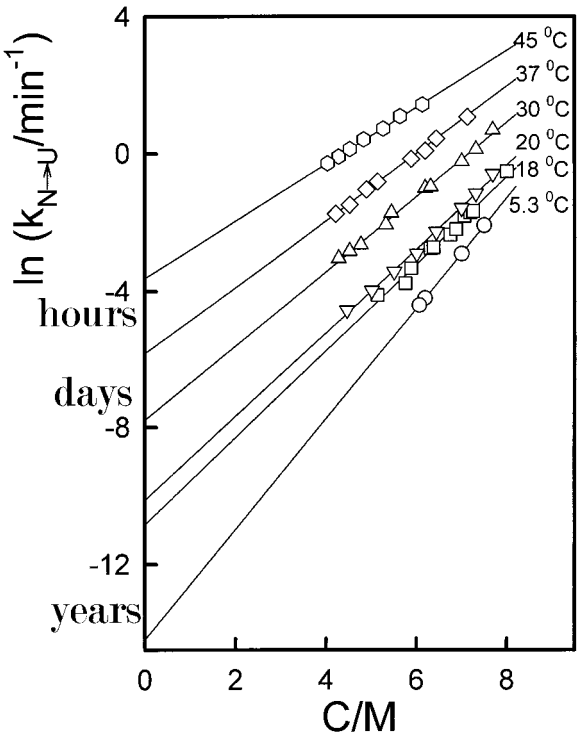

Fig. 1. Unfolding branches of Chevron plots for lysozyme unfolding in guanidinium chloride solutions, at pH 4.5, 50 mM AcNa and at the several temperatures shown. C stands for the guandinium chloride concentration. Data at 45°C, 37°C, 30°C, and 18°C are taken from Ibarra-Molero and Sanchez-Ruiz.[11] The additional data shown for 20°C and 5.3°C were obtained for this work by using fluorescence kinetic measurements as described in Ibarra-Molero and Sanchez-Ruiz.[11] For illustration, we indicate the positions in the y-axis of the unfolding rate constant values corresponding to half-lives for unfolding of the order of hours, days, and years.

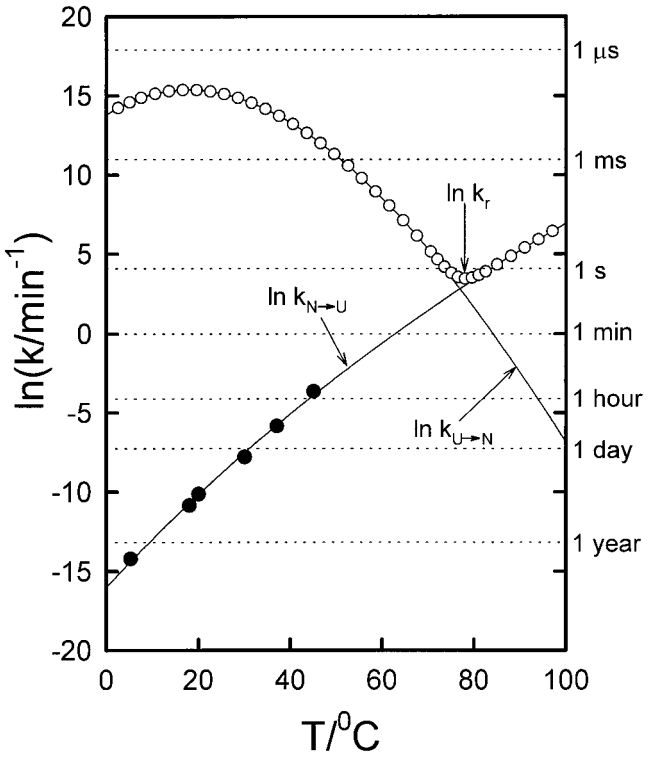

Fig. 2. Temperature dependence of the unfolding and refolding rate constants for lysozyme. The closed symbols (●) represent the values for the unfolding rate constant determined by extrapolation to zero denaturant concentration of the unfolding branches of Chevron plots (see Fig. 1) The continuous lines are the temperature dependencies of the unfolding and refolding rates given by Eqs. 9–11 and the parameters shown in Table I. The open symbols (○) represent the calculated values of the relaxation rate constant for folding-unfolding ($k_r = k_{N\to U} + k_{U\to N}$). For illustration, the positions of representatives half-life values have been indicated in the right y-axis.

important to note that we have used in our simulations physically realistic temperature-dependent values for the folding and unfolding rate constants ($k_{U\to N}$ and $k_{N\to U}$) derived from actual experimental data. This is, in fact, a key point in the theoretical analysis presented here; therefore, in the next section we describe in some detail the calculation of the folding and unfolding rate constants.

Calculation of the Rate Constants for Folding and Unfolding to Be Used in the Lumry-Eyring Simulations

The procedure we used to obtain $k_{U\to N}$ and $k_{N\to U}$ is best illustrated with HEW lysozyme. Figure 1 shows plots of rate constant for lysozyme unfolding ($k_{N\to U}$) versus guanidine concentration for several temperatures (i.e., Fig. 1 shows the unfolding branches of the Chevron plots). Some of the data in Figure 1 have been taken from our previous work,[11] but additional experimental data (not published previously) have been included (see legend to Fig. 1 for details).

Values of $k_{N\to U}$ for lysozyme in the absence of guanidine are then obtained by linearly extrapolating to zero denaturant concentration the unfolding branches of the Chevron plots, as is shown in Figure 1. We are well aware, of course, that this extrapolation is a long one and that deviations from linearity in plots of unfolding (or activation) Gibbs energy versus guanidine concentration may occur at low denaturant concentration.[11,52] Clearly, the linear extrapolation method (LEM) only yields here approximate, although physically reasonable values for $k_{N\to U}$ in the absence of guanidine; these approximate values, nevertheless, suffice for our purposes.

The temperature dependence of $k_{N\to U}$ (required by Eqs. 4 and 5) was described by the Arrhenius equation,

$$k_{N\to U} = \exp\left(-\frac{E_{N\to U}}{R}\left(\frac{1}{T}-\frac{1}{T^*}\right)\right) \qquad (9)$$

that best fitted the $k_{N\to U}$ values at several temperatures obtained using the linear extrapolation described above (see Fig. 2); the values for the unfolding activation energy ($E_{N\to U}$) and the temperature at which $k_{N\to U} = 1$ min^{-1} (T^*) derived from the fitting are shown in Table I. Note that the Arrhenius equation is, to a good approximation, equivalent to an Eyring equation with a zero activation heat capacity (the activation energy being then equal, to a good degree of approximation, to the activation enthalpy of

the Eyring equation). Actually, activation heat capacities for protein unfolding are often small, but not strictly zero.[53] However, the Arrhenius equation provides an excellent description of the our $k_{N\rightarrow U}$ for lysozyme (Fig. 2) and, in any case, a more refined analysis is not justified in this case, given the uncertainties involved in the linear extrapolation procedure.

Once the values of $k_{N\rightarrow U}$ are determined, the rate constant for lysozyme folding as a function of temperature (required by Eqs. 4 and 5) can be calculated as

$$k_{U\rightarrow N} = \frac{k_{N\rightarrow U}}{K} \tag{10}$$

using values for the equilibrium unfolding constant ($K = [U]_{EQ}/[N]_{EQ}$) obtained from:

$$-RT\cdot \ln K = \Delta H_m \cdot \left(1 - \frac{T}{T_m}\right) + \Delta C_p \times \left[T - T_m - T\cdot \ln\left(\frac{T}{T_m}\right)\right] \tag{11}$$

with the values of ΔH_m, ΔC_p and T_m given in Table I.

The procedure we used to calculate folding and unfolding rate constants for CI-2 and barnase under the solvent conditions given in Table I is essentially that described above for lysozyme. Thus, values of $k_{N\rightarrow U}$ at several temperatures and at 6M guanidine (for CI-2) or 7.25 M urea (barnase) were obtained from Figure 3 of Matouscheck et al.[54] The $k_{N\rightarrow U}$ values were then extrapolated to 0 M denaturant on the basis of LEM and the kinetic m values given in Table 3 of Matouscheck et al.,[54] and the $k_{N\rightarrow U}$ values were calculated by using Eqs. 10 and 11. The relevant parameters for barnase and CI-2 are given in Table I.

Some Comments on the Calculated Folding and Unfolding Rate Constants

Figure 2 shows the temperature dependencies of the folding and unfolding rate constants calculated for HEW lysozyme as described above (similar results were obtained for barnase and CI-2). Given the several approximations involved in the calculation (long linear extrapolation to zero denaturant concentration, zero heat capacity of activation for unfolding) the values in Figure 2 are rough estimates of $k_{U\rightarrow N}$ and $k_{N\rightarrow U,}$ suitable for the illustrative purpose of the simulations described below. Nevertheless, some comments on these values seem appropriate here.

First, the strong curvature observed in the plot of logarithm of $k_{U\rightarrow N}$ versus temperature is attributed to the large (in absolute value) activation heat capacity for folding (note that because we assumed a zero activation heat capacity for the unfolding process, the activation heat capacity for the refolding process must be equal to minus the equilibrium unfolding heat capacity change; see Scalley and Baker[55] for an equivalent interpretation of the temperature dependence of protein folding rates).

It is also interesting to note that our rough estimates of $k_{U\rightarrow N}$ correspond to half-life times for refolding at room temperature of approximately milliseconds or even lower; the reason for this is that the refolding rate constants calculated through the use of Eq. 10 necessarily correspond to the folding in the absence of significantly populated intermediates (i.e., they are the values we would obtain by extrapolating to zero denaturant concentration the region of the folding branches of the Chevron plot in which deviations caused by intermediates are not yet apparent; see Fig. 3 in Kiefhaber[10] for an example of such kind of Chevron plot). Actually, experimental refolding experiments[10,56] show that, under native conditions, most lysozyme molecules fold in a slower timescale (about 1 s) via a significantly populated intermediate (or, strictly speaking, an ensemble of intermediates of similar structure), whereas 5–10 % of lysozyme fold in a faster channel (in less than a few milliseconds) in which that intermediate is not populated; in fact, it appears[57,58] that the intermediates populated in the slow refolding channel are characterized by non-native interactions of tryptophan residues, and they might perhaps be considered as "kinetic traps," which slow down folding and which are avoided by a small fraction of molecules that, consequently, fold in a faster timescale. It should be clear, therefore, that our thermal denaturation simulations (next section) use the fast rates expected for the refolding in the absence of intermediates. Nevertheless, the effect of the intermediate states will be specifically discussed further below.

Finally, we also show in Figure 2 the temperature dependence of the rate constant that describes the relaxation to the folding-unfolding equilibrium, i.e., $k_r = k_{U\rightarrow N} + k_{N\rightarrow U}$. Note that the fact that the unfolding process is slow at temperatures well below T_m does not mean that the kinetics of relaxation is slow (k_r is the sum of the forward and reverse rate constants and, at temperatures below T_m, $k_{U\rightarrow N} >> k_{N\rightarrow U}$, $k_r \approx k_{U\rightarrow N}$ and $k_{U\rightarrow N}$ is large below T_m). Likewise, the fact that $k_{U\rightarrow N}$ is low at temperatures well above T_m does not imply that the folding-unfolding equilibrium is established slowly at those temperatures (for $T >> T_m$, we have that $k_r \approx k_{N\rightarrow U}$ and $k_{N\rightarrow U}$ is large now). In fact, the plot of k_r versus temperature shows a minimum at a temperature close to the T_m value; thus, for lysozyme (see Fig. 2) the folding-unfolding equilibrium is expected to be established in a timescale of seconds at the T_m and even faster at lower or higher temperatures (we have obtained similar results for barnase and CI-2). This result clearly disfavors the interesting proposal of Pothekin and Kovrigin[59] that experimental instances irreversibility might be caused by the kinetic trapping of the unfolded state because of the slowness of the establishment of the folding-unfolding equilibrium.

Results of the Theoretical Lumry-Eyring Simulations

Theoretical simulations were based on the numerical integration (using the MLAB environment: Civilized Software, Inc.) of the system of differential equations given by Eqs. 4–6, with the temperature dependencies of $k_{N\rightarrow U}$ and $k_{U\rightarrow N}$ given by Eqs. 9–11, together with the parameters of Table I. Integration was started from a low temperature at

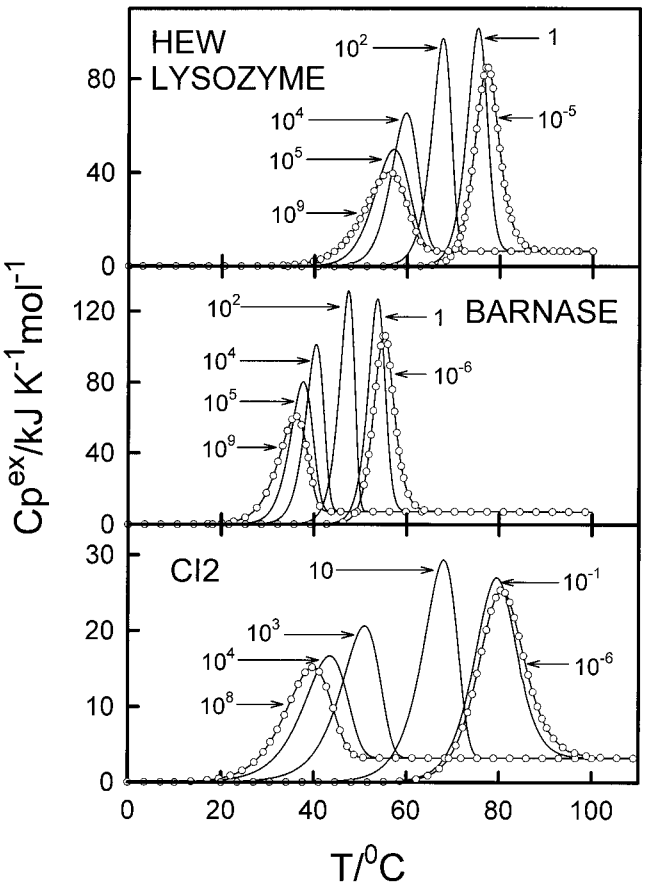

Fig. 3. DSC transitions (scanning rate 1 K/min) predicted theoretically for the denaturation of the three proteins indicated in an environment in which irreversible alterations of the unfolded state may occur. The numbers alongside the transitions stand for the rate constant of irreversible alteration in min^{-1}. For the sake of clarity, the transitions corresponding to the highest and lowest $k_{U\to F}$ values used are shown with open symbols.

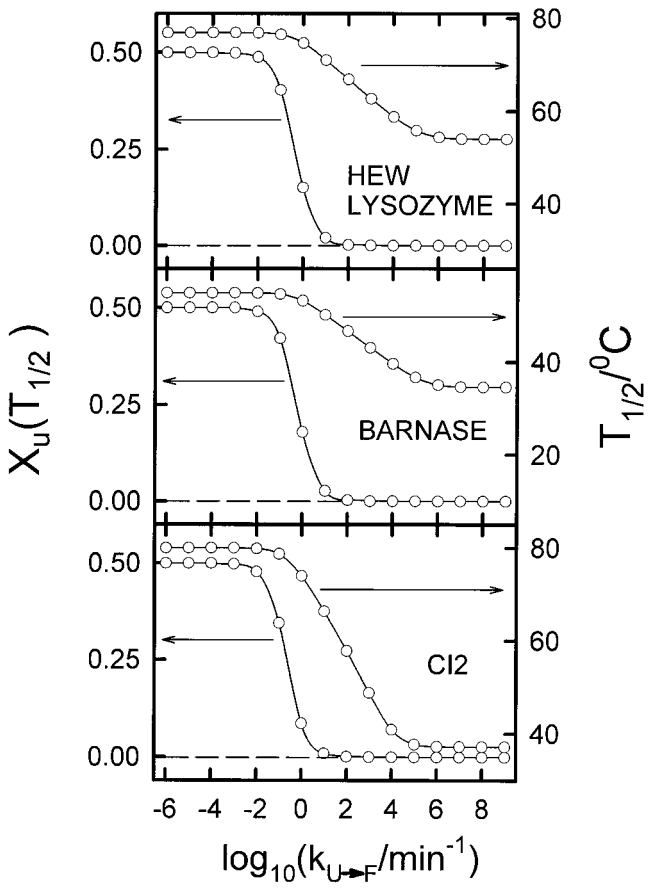

Fig. 4. Plots of denaturation temperature ($T_{1/2}$, temperature at which $X_N = 1/2$) and population of unfolded state (X_U) at $T_{1/2}$ versus the value of the rate constant for the irreversible denaturation step. The values in this figure have been obtained from theoretical simulations such as those shown in Figure 3.

which the rate of overall irreversible denaturation is negligible, and the amount of unfolded state in equilibrium with the native protein can be neglected. The resulting profiles of populations of states versus temperature were used to calculate DSC profiles using Eq. 7 with the temperature-dependent ΔH value given by Eq. 8 and the parameters of Table I.

For the three proteins under study, simulations were performed by using different values for the rate constant of the irreversible step ($k_{U\to F}$) and the resulting DSC profiles are shown in Figure 3. To bring out the main features of the corresponding populations of states versus temperature profiles, we show in Figure 4 the values of X_U at the temperature $T_{1/2}$ of each profile (temperature at which half of the protein has denatured: $X_N = X_U + X_F = 1/2$) versus the value of $k_{U\to F}$ used in the simulation. Note that the fact that $X_U \approx 0$ at $T_{1/2}$ indicates that only the native and final states are significantly populated and, consequently, that denaturation follows the two-state irreversible model. Plots of $T_{1/2}$ versus $k_{U\to F}$ are also shown in Figure 4.

The same general pattern is observed in Figures 3 and 4 for the three proteins. Thus, for values of $k_{U\to F}$ lower than (roughly) 1 min^{-1}, the predicted DSC transitions agree with those calculated, assuming that the irreversible step does not take place. For higher $k_{U\to F}$ values, the DSC transitions begin to shift to lower temperatures and, for sufficiently high $k_{U\to F}$ values, the population of unfolded state during the transition is very small and the DSC transitions fulfill all the "traditional" tests for the two-state irreversible model.[2,38] Finally, when the irreversible step is sufficiently fast, the DSC transitions become insensitive to the value $k_{U\to F}$ (i.e., they no longer shift to lower temperatures upon increasing $k_{U\to F}$). The overall behavior is illustrated by the plots of $T_{1/2}$ versus $\log_{10} k_{U\to F}$ shown in Figure 4: for the three proteins studied $T_{1/2}$ reaches a plateau at high $k_{U\to F}$ values.

Steady-State Interpretation of the Results of the Lumry-Eyring Simulations

The results described above can be understood in a very simple manner. When X_U is very low (two-state irreversible model holds), the rate of the overall denaturation

process may be described phenomenologically by an apparent first-order rate constant,

$$\frac{dX_F}{dT} = -\frac{dX_N}{dT} = \frac{k_{ap}}{\nu} X_N \tag{12}$$

and, in addition, we can apply the steady-state approximation to the unfolded protein; that is, we set $dX_U/dT = 0$ in Eq. 5, solve for X_U and substitute into Eq. 6. Then, comparison of the resulting expression with Eq. 12 yields the apparent constant in terms of the microscopic rate constants of the model:

$$k_{ap} = \frac{k_{N\to U}}{k_{U\to N} + k_{U\to F}} k_{U\to F} = \frac{Kk_{U\to F}}{1 + \frac{k_{U\to F}}{k_{U\to N}}} \tag{13}$$

There are two limiting cases of this expression, depending on whether the unfolded state "prefers" to refold or to undergo the irreversible alteration. Thus, if folding is faster than the irreversible alteration of the unfolded state ($k_{U\to N} >> k_{U\to F}$), we have that,

$$k_{ap} \approx Kk_{U\to F} \tag{14}$$

and the rate of the overall denaturation process (given by k_{ap}) is faster, the faster the irreversible step. This type of result is often referred to in Chemical Kinetics textbooks as "preliminary equilibrium kinetics," because it can be obtained by assuming that processes that occur before the rate-determining step are at equilibrium.

On the other hand, if the irreversible alteration is faster than the folding ($k_{U\to F} >> k_{U\to N}$), Eq. 13 reduces to,

$$k_{ap} \approx k_{N\to U} \tag{15}$$

and the rate of the overall denaturation process (and, therefore, the calculated DSC transitions and, in general, the operational stability of the protein) becomes independent of the rate of the irreversible step. This result is reasonable; as long as irreversible processes act mainly on the unfolded state (or non-native states, in general), the overall rate of denaturation cannot be faster than the rate of unfolding.

It is important to note that, according to Eqs.13–15, the rate constant for overall irreversible denaturation (k_{ap}) changes strongly with temperature, even if the rate constant for the irreversible step ($k_{U\to F}$) does not. Thus, under the "preliminary equilibrium" regimen the strong temperature dependence of k_{ap} is guaranteed by the presence of the unfolding equilibrium constant in Eq. 14 (i.e., if $k_{U\to F}$ is temperature independent, then the temperature dependence of k_{ap} is described, within a narrow temperature range, by an Arrhenius equation with an activation energy equal to the unfolding enthalpy). In addition, under conditions in which Eq. 15 holds, k_{ap} will change with temperature as given by the activation energy for unfolding (which is usually of the order of hundreds of kJ/mol).

Definition of Protein Stability

There has been a tendency in literature to "define" protein stability by a single parameter. Thus, in fundamental studies on folding energetics protein stability is often implicitly equated to the unfolding Gibbs energy at a given reference temperature (25°C, usually). We previously pointed out,[60] however, that what really matters for many practical and technological applications is the denaturation temperature and noted that there is no general correlation between unfolding Gibbs energy at 25°C and thermodynamic denaturation temperature; for instance, it is well known[61] that small proteins often show high denaturation temperature values, despite having low values for the unfolding Gibbs energy at room temperature (compared with the values for larger proteins); the reason for this is that the protein stability curve (the profile of unfolding Gibbs energy vs. T; see Becktel and Schellman[62]) is often flatter for small proteins, because of the small values for the unfolding entropy and heat capacity changes (see Alexander et al.[61] for details). Yet, an additional factor must be introduced in the discussion on protein stability to take into account the effect of irreversible alterations: the timescale. Thus, if irreversible processes are fast enough within the relevant timescale, the protein will be found to denature significantly at temperatures below the thermodynamic denaturation temperature. Therefore, we believe that it will prove useful to define operational protein thermal stability as the lower temperature at which significant denaturation (loss of native state) occurs in the relevant timescale. As we pointed out in the Introduction, what the relevant timescale is may depend on the case of interest (of the order of minutes, for the typical in vitro DSC experiment; the time that the enzyme is required to remain active in the reactor for some technological applications; perhaps months, if we are considering the shelf-life of a protein pharmaceutical; likely the half-life for protein degradation if we are discussing protein stability in vivo). The definition of operational protein stability we have given can be made quantitative by specifying exactly the timescale (1 min, 1 month, etc.) and what we understand by significant denaturation (50% of the protein is denatured, for instance); however, that level of precision is not required for our subsequent discussion (next section).

Upper and Lower Limits to Protein Stability

If we accept the definition of operational stability given above, then the plots of $T_{1/2}$ versus $k_{U\to F}$ of Figure 4 simply describe the effect of the rate of the irreversible alteration step on operational stability for a given timescale (the DSC time scale: minutes) and show that there is an upper limit and a lower limit to the operational stability of a given protein:

The upper limit is determined by the unfolding thermodynamics, i.e., by the unfolding Gibbs energy versus temperature profile (the protein stability curve) and is described by the equilibrium denaturation temperature (temperature at which the unfolding Gibbs energy change is zero). The upper limit is experimentally achieved when irreversible processes do not occur significantly within the relevant timescale. In in vitro thermal denaturation experiments (e.g., DSC) the upper limit was observed for some

proteins (often, low molecular weight model proteins) that undergo reversible, equilibrium denaturation. Note that these in vitro experiments involve a comparatively short timescale.

The lower limit is determined by the unfolding kinetics, i.e., by the profile of unfolding rate constant versus temperature (or by the profile of activation Gibbs energy for unfolding vs. temperature) and can be described by the temperature at which the half-life for unfolding is comparable with the relevant timescale. The lower limit is experimentally achieved when irreversible processes are fast enough, so that irreversible denaturation occurs significanly within the relevant timescale and, in addition, the unfolding is the rate-determining step of the overall irreversible denaturation process.

Transition From Preliminary Equilibrium Kinetics to the Lower Limit

According to our simulations (Figs. 3 and 4), the lower limit is reached for very high values of the rate constant for the irreversible alteration step ($k_{U\rightarrow F}$ in the Lumry-Eyring model). It must be noted, however, that, for the sake of simplicity and illustration, we based our simulations in the simplest form of the Lumry-Eyring model (Eq. 1) in which unfolding is rate limiting when the rate of irreversible alteration of the unfolded state becomes faster than its rate of refolding (see Eqs. 13 and 15); as we have already explained, the values we are using for $k_{U\rightarrow N}$ correspond to the refolding in the absence of significant populated intermediates and are very high. As a result, the change in rate determining step takes place at very high values of $k_{U\rightarrow F}$.

Actually, the situation changes if we adopt the more general view of the Lumry-Eyring model embodied in Eq 2: $N\leftrightarrow$\{Non-native ensemble\}$\rightarrow F$, where the non-native ensemble includes unfolded states and "intermediate" states (partially folded and misfolded states). Assume that, under certain conditions that favor the native state (native conditions), a given intermediate state (I) is the most populated "member" of the non-native ensemble; then, the Lumry-Eyring model would be,

$$N \leftrightarrow I \rightarrow F \tag{16}$$

and application of the steady-state approximation to I yields the following expression for the apparent rate constant for overall irreversible denaturation:

$$k_{ap} = \frac{k_{N\rightarrow I}}{k_{I\rightarrow N} + k_{I\rightarrow F}} k_{I\rightarrow F} \tag{17}$$

which should be compared with Eq. 13. The rate of the process $N\rightarrow I$ is expected to be determined by the Gibbs energy barrier between the native state and the non-native ensemble, i.e., the Gibbs energy barrier for unfolding; thus, the value of $k_{N\rightarrow I}$ in Eq. 17 may be taken as equal to the value of $k_{N\rightarrow U}$ as estimated by extrapolating to zero denaturant concentration the unfolding branches of Chevron plots. On the other hand, we may expect the rate of refolding of the intermediate ($k_{I\rightarrow N}$ in Eq. 17) to be significantly slower than the rate of "direct" refolding ($k_{U\rightarrow N}$ in Eq. 13); thus, the latter rate constant corresponds to the extrapolation to zero denaturant concentration of the folding branch in the Chevron plot, whereas the presence of significantly populated kinetic intermediates in the refolding under native conditions is often detected as a downward deviation from linearity in the folding branch (as an illustrative example, see Fig. 3 in Kiefhaber[10]); therefore, to the extent that the intermediate state that undergoes the irreversible alteration resembles a kinetic intermediate, we may expect that $k_{I\rightarrow N} < k_{U\rightarrow N}$. Now, the lower limit ($k_{ap} \approx k_{N\rightarrow I} = k_{N\rightarrow U}$) is reached when the rate of irreversible alteration is faster than the rate of refolding: $k_{U\rightarrow F} >> k_{U\rightarrow N}$ in Eq. 13 and $k_{I\rightarrow F} >> k_{I\rightarrow N}$ in Eq. 17; therefore, if the irreversible alteration occurs from an intermediate state, lower values of the rate of irreversible alteration are required to reach the lower limit (because $k_{I\rightarrow N} < k_{U\rightarrow N}$).

Again, the above ideas can be illustrated by using lysozyme as an example. Extrapolation of folding branches of Chevron plots indicates that $k_{U\rightarrow N}$ for lysozyme is of the order of 1 ms^{-1} or lower (which is consistent with our calculated values; see Fig. 2). In fact, in refolding experiments at low denaturant concentration, around 10% of lysozyme molecules appear to fold in the millisecond time scale[10]; however[56], most lysozyme molecules (around 90%) fold in slower time scale (about 1 s) through a significantly populated intermediate (strictly speaking, an ensemble of structurally related intermediates). As we have already mentioned, a plausible explanation for this slow rate of refolding could be that the intermediate is a kinetic trap in which non-native interactions are present; in fact, fluorescence studies suggest that the intermediate in lysozyme refolding is characterized by non-native interactions of the tryptophan residues.[57,58] We show in Figure 5 the plots of apparent rate constant for irreversible denaturation (k_{ap}) versus the rate constant for irreversible alteration ($k_{U\rightarrow F}$ or $k_{I\rightarrow F}$) calculated for lysozyme under the two scenarios we have discussed: (a) irreversible alterations occur directly from the unfolded state and (b) irreversible alterations occur from an intermediate state which resembles the kinetic intermediate detected in the refolding pathway under native conditions. It is clear that, in the second case, the lower limit ($k_{ap} \approx k_{N\rightarrow I} = k_{N\rightarrow U}$) is reached for much lower values of the rate constant for irreversible alteration.

The above reasonings lead us to believe that the lower limit may be fairly common in practical situations. Of course, the two-state irreversible model (Eq. 2) is consistent with both preliminary equilibrium kinetics and lower limit. We must note, however, that for the sake of simplicity, we assumed in our theoretical simulations and analyses that irreversible alterations ($U\rightarrow F$, $I\rightarrow F$) follow first-order kinetics, whereas some common irreversible alterations in vitro (aggregation, autolysis) are expected to be non-first-order kinetic processes. Thus, the fact that in experimental in vitro instances of two-state irreversible denaturation, the kinetics of the overall denaturation process is first-order argues against the irreversible step

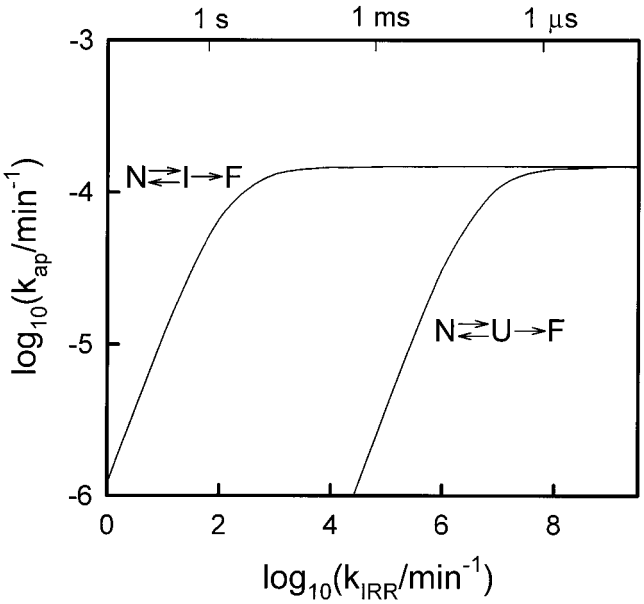

Fig. 5. Plots of overall rate constant of irreversible denaturation (k_{ap}) versus the rate constant for the irreversible step for lysozyme at 25°C. The dependencies shown have been calculated assuming that the state undergoing the irreversible process is the unfolded state ($N \leftrightarrow U \rightarrow F$) and an intermediate state with a rate constant for refolding of 2 s^{-1} ($N \leftrightarrow I \rightarrow F$). See text for details.

itself being rate determining (as is the case in the preliminary equilibrium mechanism) and suggest that the unfolding kinetics (which is first-order) determines the overall rate of denaturation and, therefore, that the lower limit has been reached.

Protein Stability In Vivo

It appears reasonable to assume that proteins are designed by evolution to have "sufficient" stability under physiological conditions. Thus, we may expect the unfolding Gibbs energy change to be positive under physiological conditions to guarantee that the native state is thermodynamically stable with respect to the unfolded protein (see, however, the discussion below). It is interesting to note, nevertheless, that unfolding Gibbs energy changes determined from experiment are indeed positive, but not too large (less than half a kJ per mole of residue, usually), which suggest that a comparatively low thermodynamic stability may be advantageous, and, in fact, several explanations for this have been adduced (some of them are reviewed in Doig and Williams[48]).

However, in addition to thermodynamic stability, many proteins must also be designed to have significant kinetic stability when confronted with the destabilizing effect of irreversible alterations. The reasons for this have already been given in earlier sections of this article, but we summarize them here: (a) because of the possibility of occurrence of irreversible alterations, thermodynamic stability (a positive value for the unfolding Gibbs energy) does not guarantee that the protein will remain in the native, biologically functional state, in a given timescale; this is strongly suggested not only by the theoretical simulations given in this work, but, mainly, by the large number[18–46] of in vitro, experimental DSC studies in which protein thermal denaturation is found to conform acceptably to the two-state irreversible model. (b) Furthermore, irreversible alterations of non-native proteins are more likely to occur in vivo than in vitro, because some irreversible processes (e.g., aggregation, "undesirable" interactions with other macromolecular components, and proteolysis) are expected to be fast in the crowded cellular environment and because in many cases, the relevant timescale in vivo will be longer than the timescale for the typical in vitro experiments (for a DSC experiment, the timescale is of the order of minutes, whereas the timescale in vivo is likely to be related to the half-life for protein degradation, which, in some cases is of the order of days or longer; see Creighton[47]).

According to the above point of view, the fact that in vitro irreversible thermal denaturation, as monitored by DSC, usually occurs above room temperature, could simply reflect that the studied proteins are "designed" to have a significant kinetic stability at physiological temperatures, so that higher temperatures are required to bring the half-life of the overall irreversible denaturation ($1/k_{ap}$) within the DSC timescale (minutes).

The Lumry-Eyring simulations reported in this work suggest the simplest way in which a protein can achieve kinetic stability when faced with irreversible alterations. Thus, there is a lower limit to the operational stability of a given protein, which means that the rate of overall irreversible denaturation cannot be faster than the rate of unfolding and, therefore, that a sufficiently high kinetic barrier for unfolding (i.e., a high kinetic barrier separating the native state from the non-native ensemble) would ensure the desired kinetic stability. This idea is best understood by using again HEW lysozyme as an example; this protein will exhibit a substantial kinetic stability when placed in an "aggressive" environment in which irreversible alterations of non-native states are very fast. The reason is that, no matter how fast those alterations are, the overall irreversible denaturation cannot be faster than the unfolding of the protein, which is, in fact, very slow at room temperature (see Fig. 1). Thus, the half-life for lysozyme unfolding at 20°C is about a few weeks, which means that, as long as irreversible processes affect mainly non-native states (a Lumry-Eyring scenario), the half-life for irreversible denaturation at 20°C will be about a few weeks or longer.

We want to emphasize that, although we believe that a substantial kinetic stability is a feature of many proteins (in particular, of complex protein systems such as membrane proteins, multimeric proteins, and supramacromolecular complexes), we are not claiming here that the rates of unfolding of all proteins at physiological temperature must be slow to ensure a significant kinetic stability in vivo (according to a recent review,[63] the rates of unfolding at room temperature for small monomeric proteins that fold with simple two-state kinetics are slow in many cases, though not in all cases). This obviously may not be

required in some cases; for instance, for some proteins degradation in vivo is fast, and it appears plausible that there is no evolutionary pressure to enhance kinetic stability beyond the limit set by the rate of degradation. Also, some "simple" proteins (low molecular weight soluble proteins) may perhaps not be very susceptible to irreversible alterations. Yet, in other cases, transient unfolding may be required for transport or function.

On the other hand, kinetic stability (likely a high kinetic barrier for unfolding) may be of particular relevance in the case of thermophilic proteins. These are very stable proteins that, in many cases, undergo denaturation above 100°C, i.e., at temperatures at which irreversible processes are expected to be very fast in vivo and in vitro. Moreover, it has been remarked[64] that in vitro thermal denaturation of thermophilic proteins is often irreversible and not amenable to thermodynamic analysis. Rubredoxin from the hyperthermophilic archaebacterium *Pyrococcus furiosus* provides a dramatic illustration of this situation. The equilibrium denaturation temperature (T_m in our terminology) for this protein was found by Englander and coworkers[64] to be close to 200°C on the basis of hydrogen exchange experiments. Thus, these authors determined the protein stability curve (the profile of unfolding Gibbs energy vs. temperature) at temperatures significanly lower than 200°C from the exchange rates measured for NHs that exchanged through the global unfolding mechanism under the EX2 limit; then, the stability curve was extrapolated to high temperature to obtain $T_m \approx 200$°C. This ingenious, roundabout procedure was followed because the in vitro thermal denaturation of rubredoxin is irreversible. In fact, rubredoxin undergoes irreversible denaturation at about 110°C at neutral pH and at about 70°C at pH 2 (i.e., these would be the $T_{1/2}$ values for the timescale of the in vitro denaturation experiments). Because $T_m \approx 200$°C, this means that, in the temperature range in which denaturation actually occurs, the amount of unfolded state is very small, and, therefore, the denaturation process and the stability of the protein must be under kinetic control.

In general, it appears highly probable that, in designing highly thermostable proteins, evolution has been forced to modify not only the equilibrium unfolding Gibbs energy change but also the activation Gibbs energy for unfolding. In connection with this, it must be noted that a change in unfolding Gibbs energy change can be brought about by mutations in virtually any part of the protein molecule; however, the same is not necessarily true for changes in activation Gibbs energy. Consider, for instance, a "polarized" transition state for unfolding, in which part of the structure is native-like (i.e., the transition-state ϕ values, as defined by Fersht and coworkers,[65] for mutations in that part of the structure would be close to 1) and part is unfolded (i.e., the transition-state ϕ values for mutations in that part of the structure would be close to 0). In this case, for a mutation to increase the kinetic barrier for unfolding, two conditions must be met: (a) it must be a stabilizing mutation in the usual thermodynamic sense (i.e., it stabilizes the native state with respect to the unfolded state) and (b) the mutation site must be located in the low-ϕ region of the transition-state structure (mutations in the $\phi \approx 1$ region are expected to affect in the same manner the Gibbs energies of the native and transition states, thus leaving unaltered the activation Gibbs energy).

Finally, we note that, if high kinetic barriers between protein states exist, the observed native state may not correspond to the global Gibbs energy minimum (a point already made by Baker and Agard[66] several years ago]. One could conceive an extreme case of this situation in which the unfolding Gibbs energy for a given protein under certain conditions (non-physiological?) is always negative, so that the native-state stability relies exclusively on a high kinetic barrier for unfolding; in other words, the stability of such protein would correspond to the lower limit even in the absence of irreversible processes, and its thermal denaturation would be described by the two-state irreversible model $N \rightarrow U$.

Protein Stability and Misfolding Diseases

Mutant proteins with altered protein stability have been associated with several diseases, including prion diseases[67,68] amyloid diseases[69–74] and cancer.[75] The analyses and discussions given in this work suggest the possibility that the relevant property in these cases is, in fact, the lower-limit kinetic stability of the proteins involved. This hypothesis is clearly speculative, but it appears to be supported by the fact that high kinetic barriers have been found in processes of amyloid fibril formation[70] and interconversion between the α and β conformations of a prion protein.[76] Here, we illustrate the implications of the hypothesis by using familial amyloid polyneuropathy (FAP) as an example.

Amyloid diseases are believed to be caused or related to the deposition in vivo of fibrils of 60–100 Å in width and of variable length, with a cross-β structure in which the individual β strands are oriented perpendicular to the long axis of the fibril. According to the so-called conformational change hypothesis, these amyloid fibrils are formed through the self-assembly of a protein state with non-native structure: the amyloidogenic intermediate.[72]

The relation between amyloid diseases and protein stability has been studied in some detail in the case of transthyretin (TTR). The wild-type form of this tetrameric protein is the major component of the amyloid deposits associated with senile systemic amyloidosis, whereas 1 of about 50 point mutants constitute the fibrils associated with FAP. Interestingly, the amyloidogenic mutations associated with FAP are located in a comparatively well-defined region of the protein structure; this mutational hot-spot comprises mainly the strands C and D, the so-called edge strands of the protein.[77,78] In addition, in vitro studies suggest that the FAP-associated mutations decrease the stability of TTR, both from the thermodynamic and kinetic viewpoint.[70,73,74] In particular, WT-TTR is a kinetically stable protein, having a half-life for unfolding of about 300 years at pH 7 and room temperature (estimated by extrapolation of the rate constants for denaturation determined at high guanidine concentration;

Lai et al.[70]); however, the FAP-associated variants Val-30-Met and Leu-55-Pro unfold three orders of magnitude faster.[70,73] This result suggests that the kinetic accessibility of the amyloidogenic intermediate plays a crucial role in the development of the amyolid desease, as already suggested by Kelly and coworkers.[70,73]

Here, we consider this relation between kinetic stability and amyloid disease in our general Lumry-Eyring approach. Thus, the amyloidogenic intermediate can be considered as a "member" of the non-native ensemble, which is "separated" from the native state by the activation barrier for unfolding, and the irreversible process is, in this case, the self-assembly of the amyloidogenic intermediate to form the amyloid fibrils. Furthermore, because the activation barrier for unfolding is very large in this case, it appears at least plausible to assume that the situation in vivo is close to the lower limit; that is, the rate of the overall irreversible process (amyloid fibril formation) is determined by the activation barrier for unfolding. This assumption is consistent, of course, with the fact that amyloidogenic variants of TTR unfold faster than WT[70,73], but, in addition, it leads to two interesting suggestions:

1. The hot spot defined by the amyloidogenic variants of TTR (strands C and D) reflects simply the structure of the transition state for unfolding. In other words, the mutational hot spot is not necessarily related with the structure of the amyloidogenic intermediate, but it may be the low-ϕ region of the transition state structure. The reason is, obviously, that thermodynamically destabilizing mutations will decrease the activation barrier for unfolding, only if the mutation sites are in the low-ϕ region.
2. To the extent that the transition-state structure does not change drastically with environment conditions, substances that are found to decrease the rate of TTR denaturation in in vitro unfolding experiments at high denaturant concentration could also be an inhibitors of amyloid fibril formation and, therefore, of potential therapeutical interest. It must be noted that, ideally, such substances would bind strongly to the native protein, while showing no binding to the transition state for unfolding.

ACKNOWLEDGMENTS

We thank Dr. E. Freire for helpful and insightful suggestions and also for encouragement.

REFERENCES

1. Lumry R, Eyring E. Conformation changes in proteins. J Phys Chem 1954;58:110–120.
2. Sanchez-Ruiz JM. Theoretical analysis of Lumry-Eyring models in differential scanning calorimetry. Biophys J 1992;61:921–935.
3. Freire E, van Osdol WW, Mayorga OL, Sanchez-Ruiz JM. Calorimetrically determined dynamics of complex unfolding transitions in proteins. Annu Rev Biophys Biophys Chem 1990;19:159–188.
4. Klibanov A, Ahern TJ. Thermal stability of proteins. In: Oxender DL, Fox CF, editors. Protein engineering. New York: Alan R. Liss; 1987. p 213–218.
5. Dill KA, Chan HS. From Levinthal to pathways to funnels: the "new view" of protein folding kinetics. Nature Struct Biol 1997;4: 10–19.
6. Baldwin RL. The nature of protein folding pathways: the classic versus the new view. J Biomol NMR 1995;103–109.
7. Onuchic JN, Luthy-Schulten Z, Wolynes PG. Theory of protein folding: the energy landscape perspective. Annu Rev Phys Chem 1997;48:545–600.
8. Privalov PL. Intermediate states in protein folding. J Mol Biol 1996;258:707–725.
9. Mücke M, Schmid FX. A kinetic method to evaluate the two-state character of solvent-induced protein denaturation. Biochemistry 1994;33:12930–12935.
10. Kiefhaber T. Kinetic traps in lysozyme folding. Proc Natl Acad Sci USA 1995;92:9029–9033.
11. Ibarra-Molero B, Sanchez-Ruiz JM. A model-independent, nonlinear extrapolation procedure for the characterization of protein folding energetics from solvent-denaturation data. Biochemistry 1996;35:14689–14702.
12. Ibarra-Molero B, Sanchez-Ruiz JM. Are there equilibrium intermediate states in the urea-induced unfolding of hen egg-white lysozyme? Biochemistry 1997;36:9616–9624.
13. Borelli MJ, Lee YJ, Frey HE, Ofenstein JP, Lepock JR. Cycloheximide increases the thermostability of proteins in chinese hamster ovary cells. Biochem Biophys Res Commun 1991;177:575–581.
14. Lepock JR, Frey HE, Ritchie KP. Protein denaturation in intact hepatocytes and isolated cellular organelles during heat shock. J Cell Biol 1993;122:1267–1276.
15. Borelli MJ, Lepock JR, Frey HE, Lee YJ, Corry PM. Excess protein in nuclei isolated from heat-shocked cells results from a reduced extractability of nuclear proteins. J Cell Physiol 1996;167:369–379.
16. Senisterra GA, Huntley SA, Escaravage M, et al. Destabilization of the Ca^{2+}-ATPasa of sarcoplasmic reticulum by thiol-specific heat shock inducers results in thermal denaturation at 37°C. Biochemistry 1997;36:11002–11011.
17. Obuchi K, Iwahashi H, Lepock JR, Komatsu Y. Stabilization of two families of critical targets for hyperthermic cell killing and acquired thermotolerance of yeast cells. Yeast 1998;14:1249–1155.
18. Arroyo-Reina A, Hernandez-Arana A. The thermal denaturation of stem bromelain is consistent with an irreversible two-state model. Biochim Biophys Acta 1995;1248:123–128.
19. Conejero-Lara F, Azuaga AI, Mateo PL. Differential scanning calorimetry of thermolysin and its 255–316 and 205–316 C-terminal fragments. React Funct Polymers 1997;34:113–120.
20. Conejero-Lara F, Mateo PL, Sanchez-Ruiz JM. Effect of Zn^{2+} on the thermal denaturation of carboxypeptidase B. Biochemistry 1991;30:2067–2072.
21. Conejero-Lara F, Sanchez-Ruiz JM, Mateo PL, Burgos FJ, Vendrell J, Aviles FX. Differential scanning calorimetry study of carboxypeptidase B, procarboxypeptidase B and its globular activation domain. Eur J Biochem 1991;200:663–670.
22. Galisteo ML, Sanchez-Ruiz JM. Kinetic study into the irreversible thermal denaturation of bacteriorhodopsin. Eur Biophys J 1993;22: 25–30.
23. Guzman-Casado M, Parody-Morreale A, Mateo PL, Sanchez-Ruiz JM. Differential scanning calorimetry of lobster haemocyanin. Eur J Biochem 1990;188:181–185.
24. Kendrick BS, Cleland JL, Lam X, et al. Aggregation of recombinant human interferon gamma: kinetics and structural transitions. J Pharm Sci 1998;87:1068–1076.
25. Kreimer DI, Shnyrov VL, Villar E, Silman I, Weiner L. Irreversible thermal denaturation of Torpedo californica acetylcholinesterase. Protein Sci 1995;4:2349–2357.
26. Le Bihan T, Gicquaud C. Kinetic study of the thermal denaturation of G actin using differential scanning calorimetry and intrinsic fluorescence spectroscopy. Biochim Biophys Res Commun 1993;194:1065–1073.
27. Lepock JR, Rodhal M, Zhang C, Heynen ML, Waters B, Cheng K. Thermal denaturation of the Ca^{2+}-ATPase of sarcoplasmic reticulum reveals two thermodynamically independent domains. Biochemistry 1990;29:681–689.
28. Lyubarev AE, Kurganov BI, Burlakova AA, Orlov VN. Irreversible thermal denaturation of uridine phosphorylase fom Escherichia coli K-12. Biophys Chem 1998;70:247–257.
29. Lyubarev AE, Kurganov BI, Orlov VN, Zhou HM. Two-state irreversible thermal denaturation of muscle creatine kinase. Biophys Chem 1999;19:199–204.
30. Marcos MJ, Chehin R, Arrondo JL, Zhadan GG, Villar E, Shnyrov

VL. pH-dependent thermal transitions of lentil lectin. FEBS Lett 1999;443:192–196.
31. Meijberg W, Schuurman-Wolters GK, Boer H, Sheek RM, Robillard GT. The thermal stability and domain interactions of the mannitol permease of Escherichia coli. J Biol Chem 1998;273: 20875–20794.
32. Menendez M, Rivas G, Diaz JF, Andreu JM. Control of the structural stability of the tubulin dimer by one high affinity bound magnesium ion at nucleotide N-site. J Biol Chem 1998;273:176–176.
33. Merabet EK, Walker MC, Yuen HK, Sikorski JA. Differential scanning calorimetry study of 5-enolpiruvoyl shikimate-3-phosphate synthase and its complexes with shikimate-3-phosphate and glyphosate: irreversible thermal transitions. Biophys Biochim Acta 1993;1161:272–278.
34. Morin PE, Diggs D, Freire E. Thermal stability of membrane-reconstituted yeast cytochrome c oxidase. Biochemistry 1990;29: 781–788.
35. Potekhin SA, Loseva OI, Tiktopulo EI, Dobritsa AP. Transition state of the rate-limiting step of heat denaturation of cry3A δ-endotoxin. Biochemistry 1999;38:4121–4127.
36. Saburova EA, Khechinashvili NN, Elfimova LI. Polyhydric alcohol-protein interactions. Microcalorimetry of lactate dehydrogenase denaturation in water-glycerol solutions. Molekulyarnaya Biologiya 1996;30:1219–1228.
37. Sanchez-Ruiz JM, Lopez-Lacomba JL, Mateo PL, Vilanova M, Serra MA, Aviles FX. Analysis of the thremal unfolding of porcine procarboxypeptidase A and its functional pieces by differential scanning calorimetry. Eur J Biochem 1988;176:225–230.
38. Sanchez-Ruiz JM, Lopez-Lacomba JL, Cortijo M, Mateo PL. Differential scanning calorimetry of the irreversible thermal denaturation of thermolysin. Biochemistry 1988;27:1648–1652.
39. Shnyrov VL, Marcos MJ, Villar E. Kinetic study on the irreversible thermal denaturation of lentil lectin. Biochem Mol Biol Int 1996;39:647–656.
40. Shnyrov VL, Diez-Martinez L, Roig MG, Lyubarev AE, Kurganov BI, Villar E. Irreversible thermal denaturation of lipase B from Candida rugosa. Thermochim Acta 1999;325:143–149.
41. Shnyrov VL, Zhadan GC, Cobaleda C, Sagrera A, Muñoz-Barroso I, Villar E. A differential scanning calorimetry study on Newcastle disease virus: identification of proteins involved in thermal transitions. Arch Biochem Biophys 1997;341:89–97.
42. Solis-Mendiola S, Gutierrez-Gonzalez LH, Arroyo-Reyna A, Padilla-Zuñiga J, Rojo-Dominguez A, Hernandez-Arana, A. pH dependence of the activation parameteres for chymopapain unfolding: influence of ion pairs on the kinetic stability of proteins. Biochim Biophys Acta 1998;1388:363–372.
43. Villaverde J, Cladera J, Hartog A, Berden J, Padros E, Duñac M. Nucleotide and Mg^{2+} dependency of the thermal denaturation of mitochondrial F_1-ATPase. Biophys J 1998;75:1980–1988.
44. Villaverde J, Cladera J, Padros E, Rigaud JL, Duñac M. Effect of nucleotides on the thermal stability and on the deuteration kinetics of the thermophylic F_0F_1 ATP synthase. Eur J Biochem 1997;244:441–448.
45. Zhadan GG, Shnyrov VL. Differential scanning calorimetry study of the irreversible thermal denaturation of 8 kDa cytotoxin from the sea anemone Radianthus macrodactilus. Biochem J 1994;299: 731–733.
46. Zhadan GC, Cobaleda C, Jones AL, Leal F, Villar E, Shnyrov VL. Protein involvement in thermally induced structural transitions of pig erythrocyte ghosts. Biochem Mol Biol Int 1997;42:11–20.
47. Creighton TE. Proteins, structures and molecular properties. 2nd ed. New York: Freeman and Company; 1993. Chapter 10. p 466–468.
48. Doig AJ, Williams DH. Why water-soluble, compact, globular proteins have similar specific enthalpies of unfolding at 110°C. Biochemistry 1992;31:9371–9375.
49. Lepock JR, Richtie KP, Kolios MC, Rodhal AM, Heinz KA, Kruuv J. Influence of transition rates and scan rate on kinetic simulations of differential scanning calorimetry profiles of reversible and irreversible protein denaturation. Biochemistry 1992;31:12706–12712.
50. Makhatadze GI, Privalov PL. Energetics of protein structure. Adv Prot Chem 1995;47:307–425.
51. Johnson CM, Fersht AR. Protein stability as a function of denaturant concentration: the thermal stability of barnase in the presence of urea. Biochemistry 1995;34:6795–6804.
52. Ibarra-Molero B, Loladze VV, Makhatadze GI, Sanchez-Ruiz JM. Thermal versus guanidine-induced unfolding of ubiquitin: an analysis in terms of the contributions from charge-charge interactions to protein stability. Biochemistry 1999;38:8138–8149.
53. Plaxco KW, Simons KT, Baker D. Contact order, transition state placement and the refolding rates of single domain proteins. J Mol Biol 1998;277:985–994.
54. Matouscheck A, Otzen DE, Itzhaki LS, Jackson SE, Fersht AR. Movement of the position of the transition state in protein folding. Biochemistry 1995;34:13656–13662.
55. Scalley ML, Baker D. Protein folding kinetics exhibit an Arrhenius temperature dependence when corrected for the temperature dependence of protein stability. Proc Natl Acad Sci USA 1997;94: 10636–10640.
56. Radford S, Dobson CM, Evans PA. The folding of hen lysozyme involves partially structured intermediates and multiple pathways. Nature 1992;358:302–307.
57. Denton ME, Rothwarf DM, Scheraga HA. Kinetics of folding of guanidine-denatured hen egg white lysozyme and crboxymethyl(Cys^6,Cys^{127})-lysozyme: a stopped-flow absorbance and fluorescence study. Biochemistry 1994;33:11225–11236.
58. Rothwarf DM, Scheraga HA. Role on non-native aromatic and hydrophobic interactions in the folding of hen egg white lysozyme. Biochemistry 1996;35:13797–13807.
59. Pothekin SA, Kovrigin EL. Folding under inequilibrium conditions as a possible reason for partial irreversibility of heat-denatured proteins; computer simulation study. Biophys Chem 1998;73:241–248.
60. Plaza del Pino IM, Sanchez-Ruiz JM. An osmolyte effect on the heat capacity change for protein folding. Biochemistry 1995;34: 8621–8630.
61. Alexander P, Fahnestock S, Lee T, Orban J, Bryan P. Thermodynamic analysis of the folding of the streptococcal protein G IgG-binding domains B1 and B2: why small proteins tend to have high denaturation temperatures. Biochemistry 1992;31:3597–3603.
62. Becktel WJ, Schellman JA. Protein stability curves. Biopolymers 1987;26:1859–1877.
63. Jackson SE. How do small single-domain proteins fold? Folding Design 1998;3:R81–R91.
64. Hiller R, Zhou ZH, Adams MWW, Englander SW. Stability and dynamics in a hyperthermophilic protein with melting temperature close to 200°C. Proc Natl Acad Sci USA 1997;94:11329–11332.
65. Fersht AR, Matouscheck A, Serrano L. The folding of an enzyme. I. Theory of protein engineering analysis of stability and pathway of protein folding. J Mol Biol 1992;224:771–782.
66. Baker D, Agard DA. Kinetics versus thermodynamics in protein folding. Biochemistry 1994;33:7505–7509.
67. Liemann S, Glockshuber R. Influence of amino acid substitutions related to inherited human prion diseases on the thermodynamic stability of cellular prion protein. Biochemistry 1999;38:3258–3267.
68. Horiuchi M, Caughey B. Prion protein interconversions and the transmissible spongiform encephalopathies. Structure 1999;7: R231–R240.
69. Booth DR, Sunde M, Bellotti V, et al. Instability, unfolding and aggregation of human lysozyme variants underlying amyloid fibrillogenesis. Nature 1997;385:787–793.
70. Lai Z, McCulloch J, Lashuel HA, Kelly JW. Guanidine hydrochloride-induced denaturation and refolding of transthyretin exhibits a marked hysteresis: equilibria with high kinetic barriers. Biochemistry 1997;36:10230–10239.
71. Peterson SA, Klabunde T, Lashuel HA, Purkey H, Sacchettini JC, Kelly JW. Inhibiting transthyretin conformational changes that lead to amyloid fibril formation. Proc Natl Acad Sci USA 1998;95: 12956–12960.
72. Kelly JW. The alternative conformations of amyloidogenic proteins and their multi-step assembly pathways. Curr Opin Struct Biol 1998;8:101–106.
73. Lashuel HA, Zhihong L, Kelly JW. Characterization of the transthyretin acid denaturation pathways by analytical ultracentrifugation: implications for wild-type, V30M, and L55P amyloid fibril formation. Biochemistry 1998;37:17851–17864.
74. Nettleton EJ, Sunde M, Lai Z, Kelly JW, Dobson CM, Robinson CV. Protein subunit interactions and structural integrity of

amyloidogenic thransthyretins: evidence from electrsopray mass spectrometry. J Mol Biol 1998;281:553–564.
75. Bullock AN, Henckel J, DeDecker BS, Johnson CM, Nikolova PV, Proctor MR, Lane DP, Fersht AR. Thermodynamic stability of wild-type and mutant p53 core domain. Proc Natl Acad Sci 1997;94:14338–14342.
76. Jackson GS, Hosszu LLP, Power A, Hill AF, Kenney J, Saibil H, Craven CJ, Waltho JP, Clarke AR, Collinge J. Reversible conversion of monomeric human prion protein between native and fibrilogenic conformations. Science 1999;283:1935–1937.
77. Serpell L, Blake CCF. Frequency analysis and structural correlation of FAP mutations in transthyretin. In: Kisilevsky R, Benson MD, editors. Amyloid and amyloidosis. New York: Parthenon Publishing Group Inc; 1994. p 447–450.
78. Sepell L, Goldstein G, Dackling I, Lundgreen E, Blake CCF. The "edge strand" hypothesis: prediction and test of a mutational "hot spot" on the thransthyretin molecule associated with FAP amyloidogenesis. Amylod: Int J Exp Clin Invest 1996;3:75–85.
79. Jackson SE, Fersht AR. Folding of chymotrypsin inhibitor-2. 1. Evidence for a two-state transition. Biochemistry 1991;30:10428–10435.